

# SOME PARAMETERIZATIONS OF THE NOCTURNAL BOUNDARY LAYER

K. S. RAO and H. F. SNODGRASS\*

*Atmospheric Turbulence and Diffusion Laboratory, National Oceanic and Atmospheric Administration,  
Oak Ridge, Tennessee, 37830, U.S.A.*

(Received 21 December, 1978)

**Abstract.** The evolution and structure of a steady barotropic nocturnal boundary layer are investigated using a higher-order turbulence closure model which includes equations for the mean quantities, turbulence covariances, and the viscous dissipation rate. The results indicate that a quasi-steady nocturnal PBL might be established in 4–10 hours after transition, depending on surface cooling rate. The latter is assumed to be constant in the model. The emphasis is on prediction of eddy viscosity, nocturnal mixing-layer depth, and the stability-dependent universal functions in the geostrophic drag and heat transfer relations. The model predictions are parameterized in the framework of the PBL similarity theory and compared with observations and results of other models.

## 1. Introduction

The atmospheric boundary layer is generally stably-stratified over land at night, though persistent daytime inversions also often occur in winter. The nocturnal mechanically-mixed layer is typically much shallower than the daytime convectively-mixed layer. Its depth also varies widely, from a few meters to hundreds of meters, depending on the upper wind, stability, and terrain. This has an important bearing on the dispersion of pollutants in the atmosphere; maximum pollutant-concentration levels are usually associated with strongly stable conditions and low wind speeds, when the diffusive ability of the atmosphere is at a minimum. It is important therefore to study the physical processes of the nocturnal boundary layer and develop models capable of simulating the salient features of its turbulence as well as mean profiles. The models should enable us to improve diffusion estimates for stable conditions.

Several numerical and analytical model studies of the nocturnal boundary layer have been reported in the literature. These include Deardorff (1972), Businger and Arya (1974), Delage (1974), Wyngaard (1975), Blackadar (1976), Briggs (1977), Zeman and Lumley (1978), and Brost and Wyngaard (1978).

In the present study, we use Wyngaard's (1975) higher-order turbulence closure model to investigate the steady-state structure of an idealized nocturnal planetary boundary layer (PBL). The emphasis is on prediction and parameterization of eddy viscosity, dissipation rate of turbulent kinetic energy, mixing-layer depth, and the stability-dependent universal functions in the geostrophic drag and heat transfer relations. The model predictions are parameterized in the framework of the PBL similarity theory and compared with observations and results of other models.

\* Affiliated with Oak Ridge Associated Universities (ORAU).

## 2. The Model

We consider a horizontally homogeneous barotropic PBL over a flat homogeneous surface. Neglecting the moisture effects and radiation flux divergence, the mean flow equations, with  $x$  axis in the direction of surface shear stress and  $z$  in the vertical, are

$$\begin{aligned}\partial U/\partial t &= -\partial \overline{uw}/\partial z + f(V - V_g) \\ \partial V/\partial t &= -\partial \overline{vw}/\partial z + f(U_g - U) \\ \partial \Theta/\partial t &= -\partial \overline{\theta w}/\partial z.\end{aligned}\tag{1}$$

Here  $(U, V, W = 0)$  are the mean velocity components in  $(x, y, z)$  directions, respectively, and  $\Theta$  is the mean potential temperature. The corresponding fluctuating quantities are given by  $(u, v, w)$  and  $\theta$ ;  $f$  is the Coriolis parameter; and the components of the geostrophic wind vector  $\mathbf{G} = U_g \mathbf{i} + V_g \mathbf{j}$  are defined by  $fU_g = -\partial P/\partial y$  and  $fV_g = \partial P/\partial x$ , where  $P$  is the mean kinematic pressure.

In order to solve Equation (1), we write transport equations for the turbulent fluxes of momentum and heat. These equations are closed approximately by expressing the third moments in terms of dimensionally-consistent, physically-plausible, semi-empirical expressions involving the mean quantities, the second moments, and a turbulence time scale  $\tau = 2E/\varepsilon$ , where  $\varepsilon$  is the mean viscous dissipation rate of the turbulent kinetic energy ( $E = \overline{u_i u_i}/2$ );  $\tau$  is determined by the model itself, not specified *a priori*, since the model also includes a dynamical equation for  $\varepsilon$ . These higher-order closure models are discussed by Wyngaard (1975), and reference should be made to that paper for details.

The closed equation set was numerically integrated in time on a digital computer using a Dufort–Frankel explicit finite-difference scheme. A logarithmic transformation of the vertical coordinate was used from the lower boundary, set at  $z = 1$  m, to the upper boundary at 1000 m, with a total of 51 grid points. The lower boundary conditions were based on the surface-layer flux–profile relations (Businger *et al.*, 1971) and other data from field measurements and numerical studies. At the upper boundary, a simulated inversion lid, all turbulence quantities and the vertical gradients of mean variables were set to zero.

In order to study the temporal evolution of the nocturnal boundary layer, the model was initialized with equilibrium distributions of variables in a decaying convective PBL around sunset at the instant of transition ( $t = 0$ ) when the vertical surface temperature flux ( $Q_0 = H_0/\rho c_p$ ) goes to zero. To simulate the nocturnal PBL, a constant cooling rate, ranging from 0.2 to 2.0 C hr<sup>-1</sup>, was specified at the surface ( $z_0$ ), the geostrophic wind ( $G$ ) was provided, and the surface friction velocity ( $u_*$ ), surface heat flux ( $H_0$ ), Monin–Obukhov stability length ( $L$ ), and cross-isobar angle ( $\alpha$ ) were determined from the model at each  $t$ . In the calculations, we specified westerly winds, 45 N latitude, a constant  $G = 10$  m s<sup>-1</sup> and a roughness length  $z_0 = 0.01$  m. For convenience, we used a coordinate system with the positive  $x$ -axis oriented in the direction of the geostrophic wind, and adjusted the lower boundary

conditions to account for the angle  $\alpha(t)$  between surface and geostrophic winds. Details of the computational techniques, boundary and initial conditions as well as the model equations can be found in Rao and Snodgrass (1978).

### 3. Results and Discussion

In a horizontally homogeneous nocturnal PBL with negligibly small radiation flux divergence, the cooling rate is balanced entirely by the turbulent flux divergence. For a constant surface-cooling rate, a quasi-steady state may be established when

$$\frac{\partial \Theta}{\partial t} = \frac{-\partial \overline{w\theta}}{\partial z} = Q_0/h = \text{constant}, \quad (2)$$

or

$$\frac{\partial}{\partial t} (\partial \Theta / \partial z) = \frac{-\partial^2}{\partial z^2} (\overline{w\theta}) = 0,$$

where  $h$  is the mixing-layer depth. This implies that heat flux decreases linearly with height; both  $Q_0$  and  $h$ , as well as other key PBL parameters such as  $u_*$ ,  $\alpha$  and  $L$ , should approach constant values as the PBL approaches a quasi-steady state. This leads to a near-constant value for the PBL stability parameter  $\mu = |u_*/fL|$ , where  $\mu$  represents the ratio of the rotation time scale,  $|f|^{-1}$ , to the turbulence time scale,  $L/u_*$ , in the stable case. The steady-state value of  $\mu$  increases with the surface cooling rate.

The results indicate that after an initial period of rapidly changing values, a quasi-steady nocturnal PBL, characterized by near-constant values of  $u_*$ ,  $Q_0$ ,  $L$ ,  $h$  and  $\alpha$ , might be established in 4–10 h after transition, depending on the surface cooling rate. The model predictions of the mean field and turbulence structure show good agreement with the atmospheric surface-layer observations from Kansas and Minnesota experiments (Wyngaard, 1975; Rao and Snodgrass, 1978). This idealized steady state may be short-lived in reality (see Businger, 1973, p. 86), but nevertheless is useful in understanding the equilibrium structure of the stable PBL.

#### 3.1. EDDY VISCOSITY DISTRIBUTION

The vertical distributions of eddy viscosity,  $K$ , are of considerable interest since several recent papers on the nocturnal PBL are based on the eddy viscosity models in which the stresses in the mean momentum equation (1) are replaced by

$$\overline{uw} = -K_{xz} \partial U / \partial z, \quad \overline{vw} = -K_{yz} \partial V / \partial z. \quad (3)$$

The vertical profiles of  $K_{xz}$ , plotted nondimensionally in Figure 1 show a strong dependence on the PBL stability parameter  $\mu$ . As  $\mu$  increases, the eddy viscosity profiles become flatter; both the maximum eddy viscosity,  $K_{\max}$ , as well as the height where it occurs,  $z_{\max}$ , decrease by nearly two orders of magnitude as the PBL

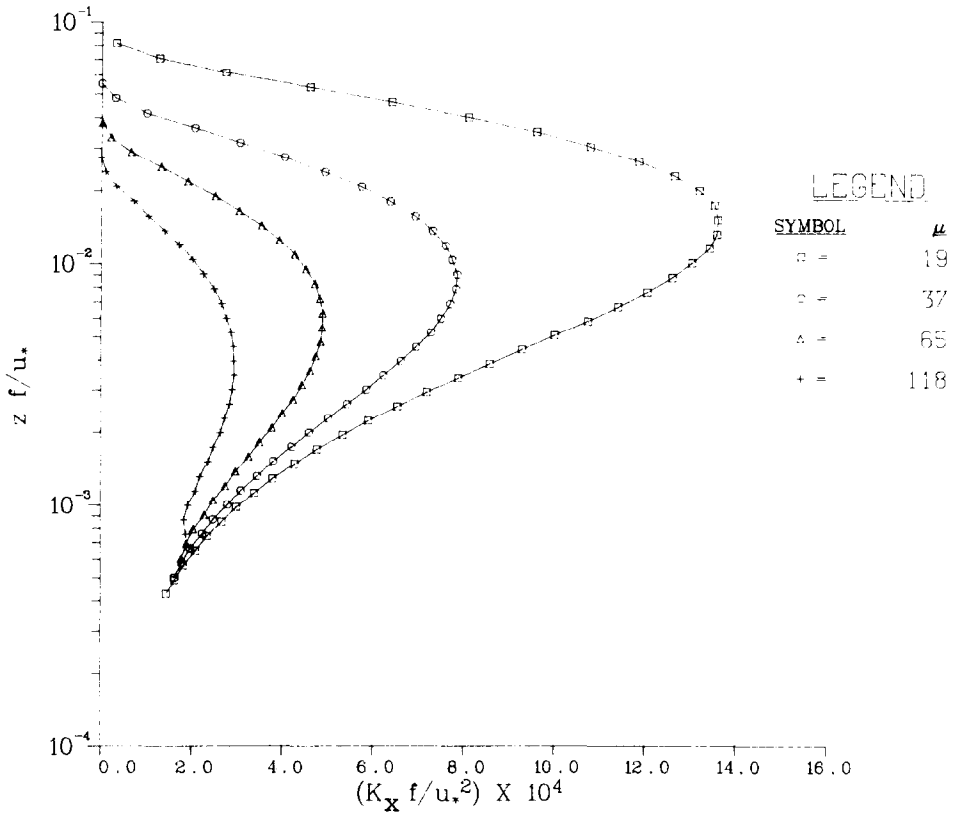


Fig. 1. Nondimensional eddy viscosity distributions in the quasi-steady nocturnal PBL, calculated for different stabilities.

changes from neutral ( $\mu = 0$ ) to moderately stable ( $\mu = 118$ ). The calculated variations of  $K_{\max}$  and  $z_{\max}$  are functions of  $\mu$ ; for  $\mu > 10$ , they are given by the best-fit expressions

$$\begin{aligned} K_{\max} f / u_*^2 &= 0.016 \mu^{-0.83} \\ z_{\max} f / u_* &= 0.168 \mu^{-0.80} \end{aligned} \quad (4)$$

In PBL models, it is often taken that  $K_{yz} = K_{xz}$  ( $= K$ , say); this assumption is consistent with our results in Figure 2, which shows identical vertical profiles of  $K_{xz}$  and  $K_{yz}$  calculated for  $\mu = 65$ . It will be useful to compare these profiles with the corresponding  $K$ -distributions used by other models based on  $K$ -theory. Businger and Arya (1974) specified steady-state eddy viscosity distributions by the implicit relation

$$\frac{Kf}{u_*^2} = \frac{k\xi}{(1 + \beta\mu\xi)} \exp\left(-\left|\frac{V_g}{u_*}\right|\xi\right), \quad (5)$$

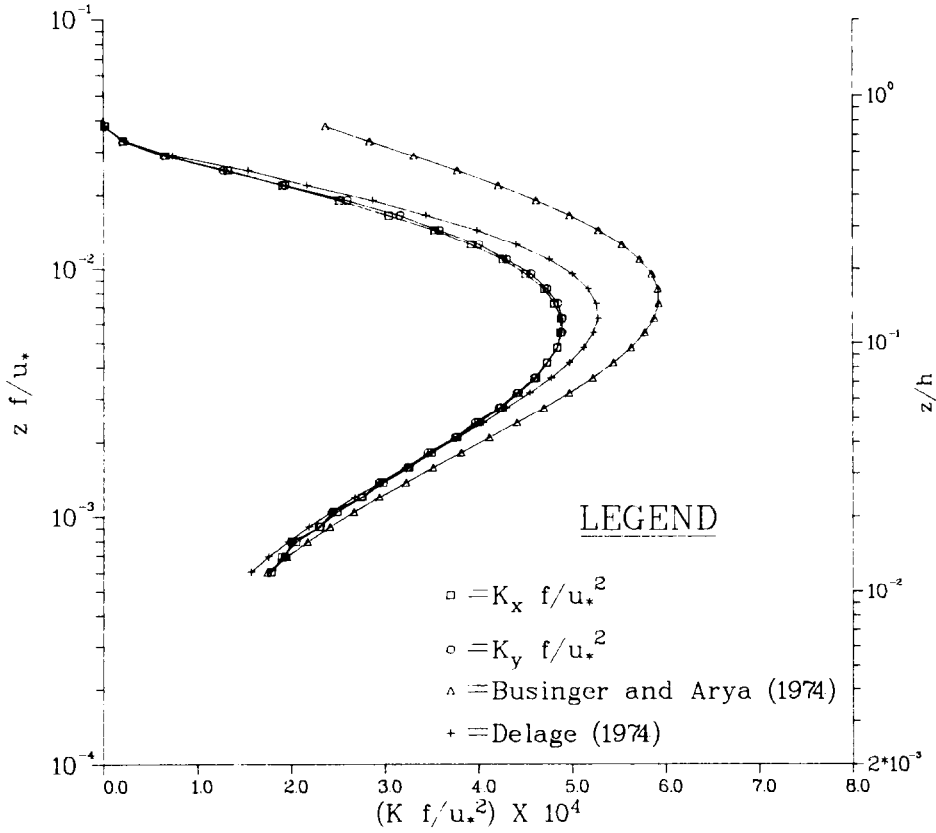


Fig. 2. Comparison of calculated nondimensional eddy viscosity profiles with those used in other nocturnal PBL models.

where  $k = 0.35$ ,  $\beta = 4.7$ ,  $\xi = fz/u_*$  and  $|V_g| = |G \sin \alpha|$ . Delage (1974) used the expression

$$K = l(0.16E)^{1/2}, \tag{6a}$$

where  $l$  is a mixing length given as

$$l = \{1/k(z + z_0) + 1/\lambda + \beta/kL'\}^{-1} \tag{6b}$$

with  $k = 0.4$ ,  $\beta = 5$ , and  $\lambda = 0.0004Gf^{-1}$ . Here  $L'(z)$  is the local value of the Monin–Obukhov stability length. Using the steady-state values of  $\alpha$ ,  $E$ , and  $L'$  calculated by the present model for  $\mu = 65$ , Equations (5) and (6) are evaluated and compared with the  $K$ -profiles in Figure 2. Equation (5) gives somewhat larger  $K$  values in the outer layer while Equation (6) agrees fairly well with our results. Both equations predict slightly higher peaks than the present model; however, the general profile shape and behaviour are similar in all models.

The  $K$ -variation shown in Figure 1 may be parameterized as  $K/u_*z = F(\zeta, \mu)$  where  $\zeta = z/L$ . The predicted steady-state eddy viscosity profiles are represented

well (see Figure 3) by

$$K = \frac{ku_*z}{(1+4.7\zeta)} e^{-b\eta}, \quad (7)$$

where  $k = 0.35$ ,  $b = 9.1$ , and  $\eta = \zeta\mu^{-1/2}$ . Using relations given later in this paper, Businger and Arya's (1974)  $K$ -expression, Equation (5), can also be reduced to this form. The advantage of Equation (7) is that the steady-state eddy viscosity profile in the nocturnal PBL can be specified explicitly from the surface-layer parameters,  $u_*$  and  $L$ .

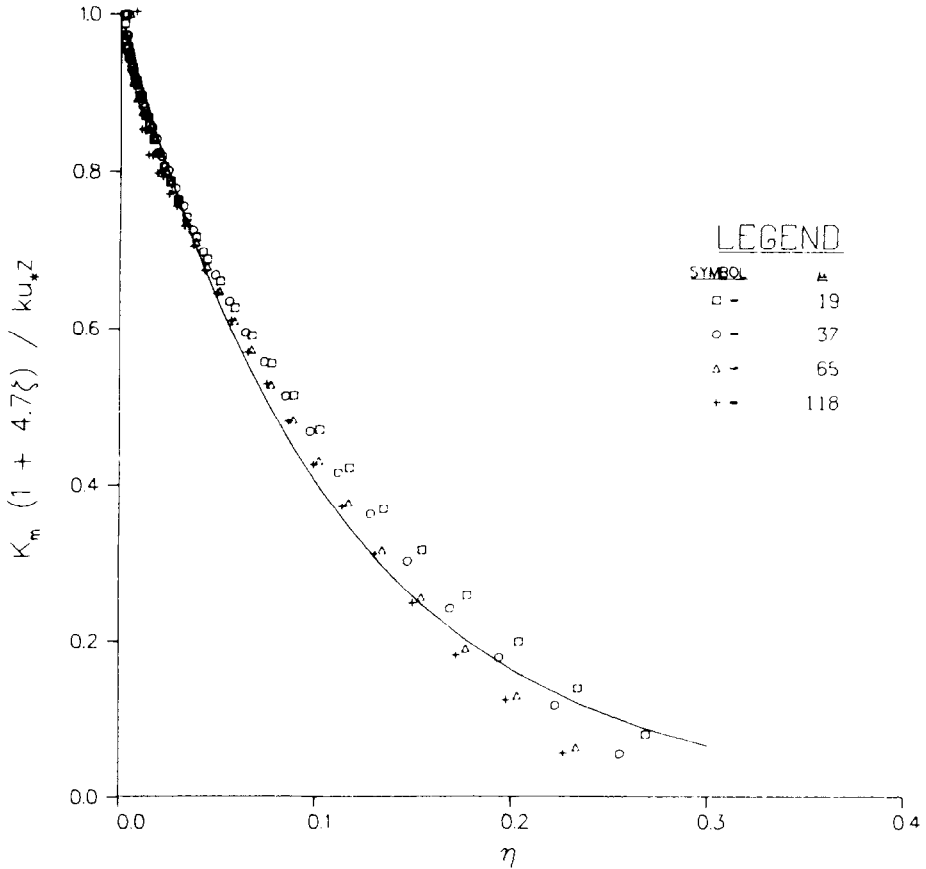


Fig. 3. Similarity representation of calculated eddy viscosity distribution in the quasi-steady nocturnal PBL. The best-fit curve (solid line) is given by Equation (7).

The dissipation rate of turbulent kinetic energy is calculated in the model by a dynamical equation for  $\epsilon$ . The steady state  $\epsilon$ -profiles in the nocturnal PBL are adequately represented by

$$\phi_\epsilon = (\phi_m - \zeta) e^{-6.5\eta}, \quad (8)$$

where  $\phi_\varepsilon = (kz/u_*^3)\varepsilon$  and  $\phi_m = (kz/u_*) [(\partial U/\partial z)^2 + (\partial V/\partial z)^2]^{1/2}$  are dimensionless dissipation rate and horizontal mean wind shear, respectively. The decrease of  $\varepsilon$  with height is in qualitative agreement with the recent Minnesota data (Caughey *et al.*, 1978).

### 3.2. NOCTURNAL MIXING-LAYER DEPTH

The variation of the nocturnal mixing-layer depth  $h$ , calculated somewhat arbitrarily as the height where the shear stress decreases to 5% of its surface value, is plotted in the dimensionless form shown in Figure 4(a). The best fit, for  $\mu > 10$ , is given by

$$h|f|/u_* = a\mu^{-1/2}, \quad \text{or} \quad h/L = a\mu^{1/2} \quad (9)$$

where  $a$  is a constant of order unity. This relation was first suggested by Zilitinkevich (1972, 1975) from similarity considerations and dimensional analysis. From Equation (9), we can write  $h \sim |u_*L/f|^{1/2}$ ; thus the nocturnal mixing-layer depth in the idealized barotropic PBL at middle latitudes is proportional to the geometric mean of the length scales  $u_*/|f|$  and  $L$ , and it is uniquely determined by the surface stress, Coriolis parameter, and stability. In the present model, calculating  $h$  as mentioned above, we evaluated  $a = 0.27$  in the steady state; the corresponding values of this constant from other models are 0.55 (Businger and Arya, 1974), 0.22 (Wyngaard, 1975), and 0.40 (Brost and Wyngaard, 1978). Thus, its value appears to be strongly dependent on some of the model parameterizations. The model results in Figure 4(a) show that the value of  $a$  also depends on  $t$ ; at  $t = 2$  h,  $a = 0.43$  and decreases to 0.27 as the flow approaches steady state.

The nocturnal boundary-layer height, determined from the temperature and wind soundings as the height to which significant surface cooling has extended, typically increases with time during the night (Blackadar, 1957; Izumi and Barad, 1963;

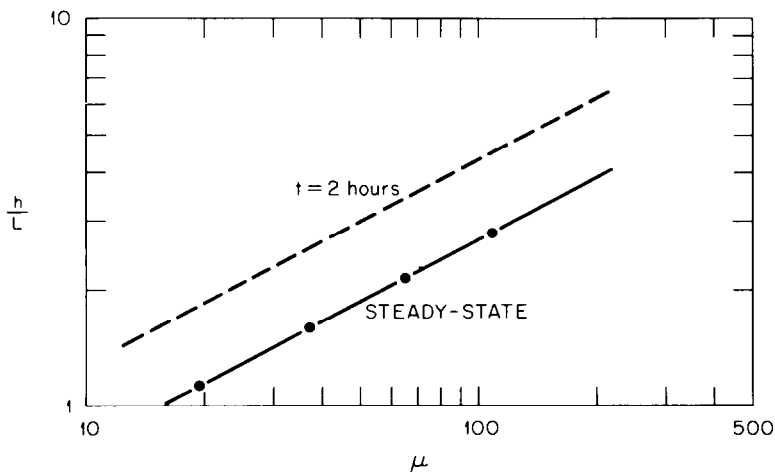


Fig. 4(a). Calculated variation of the dimensionless nocturnal mixing-layer depth as function of the stability parameter  $\mu$ . See text, Equation (9).

Deardorff, 1972). Yamada (1976) determined  $h$  as the height of the surface inversion layer from the radiosonde-measured  $\Theta_v$  profiles of the Wangara data (Clarke *et al.*, 1971), and found that under strongly stable conditions,  $h > 0.3 |u_* / f|$ , the neutral PBL height. These findings indicate that  $h$  determined from the  $\Theta_v$  profile, usually exceeds the height where turbulent shear stress and heat flux become negligible, probably due to radiative and advective effects, and may not be a good indicator of the nocturnal mixing-layer depth. It also appears that, unlike the daytime convective case, the evolution of the nocturnal PBL height cannot be satisfactorily described by a rate equation (Yu, 1978).

It is difficult to verify Equation (9) from available observations. Ideally, one would require turbulence profile measurements in the stable boundary layer under stationary, horizontally-homogeneous conditions. These conditions are rarely satisfied and turbulence data are scarce.

The Kansas surface-layer data (Izumi, 1968), in addition to  $u_*$  and  $L$ , include 15-min average measurements of  $\overline{w\theta}$  at  $z = 5.66, 11.31$  and  $22.63$  m, and the

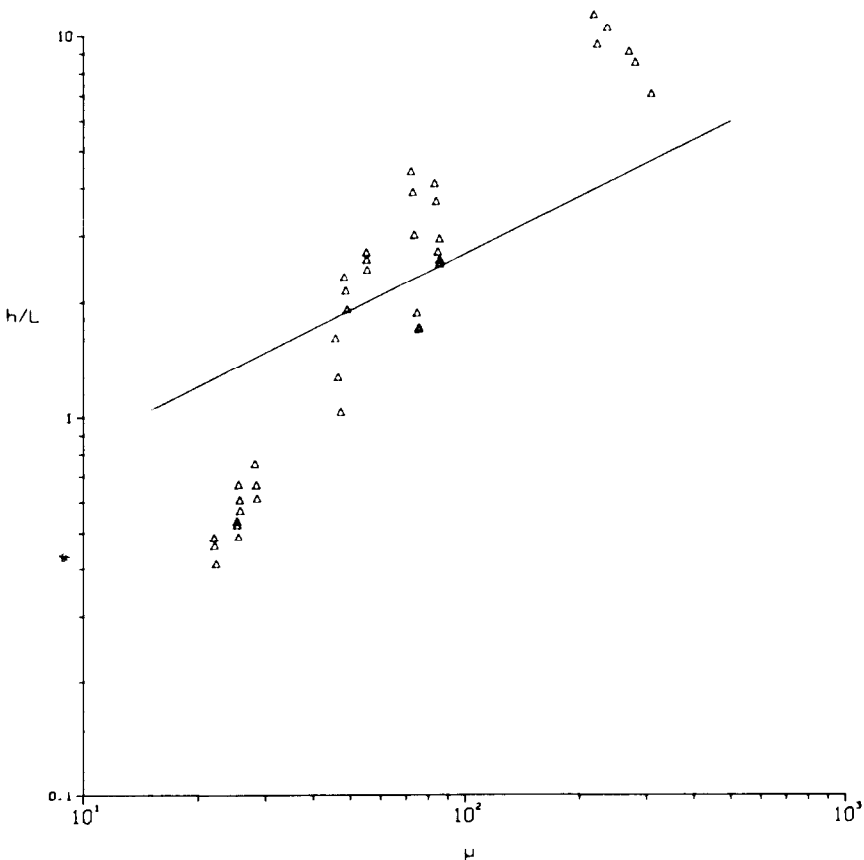


Fig. 4(b). Comparison of model prediction (solid line) with the variation of nocturnal mixing-layer depth deduced from the Kansas data. (See text for details).



corresponding potential temperature profiles which allow the determination of cooling rates at these heights. Assuming a linear decrease of heat flux with height (Wyngaard, 1975; Rao and Snodgrass, 1978) in the nocturnal mixing layer,  $h$  is then estimated from Equation (2). The variation of half-hour average estimates of  $h$  are plotted in Figure 4(b) along with the present model prediction,  $h/L = 0.27 \mu^{1/2}$ , for comparison.

A similar analysis was carried out for the Wangara stable boundary layer data (Clarke *et al.*, 1971) and the results are shown in Figure 4(c). In this case, 1-h average values of the parameters  $Q_0$ ,  $L$  and  $u_*$  are based on the calculations of Melgarejo and Deardorff (1975), and the corresponding cooling rates are estimated from screen-level (1.2 m) temperatures. The Wangara results cover a shorter range of  $\mu$  and show more scatter than the Kansas data, probably due to significant radiation flux divergence, which was not considered in the present model. It should be noted that the preceding analysis for the estimation of  $h$  is based on several assumptions, including a continuous turbulence regime in the nocturnal mixing layer and negligible advective effects, which are often not satisfied in the real atmosphere. In a recent

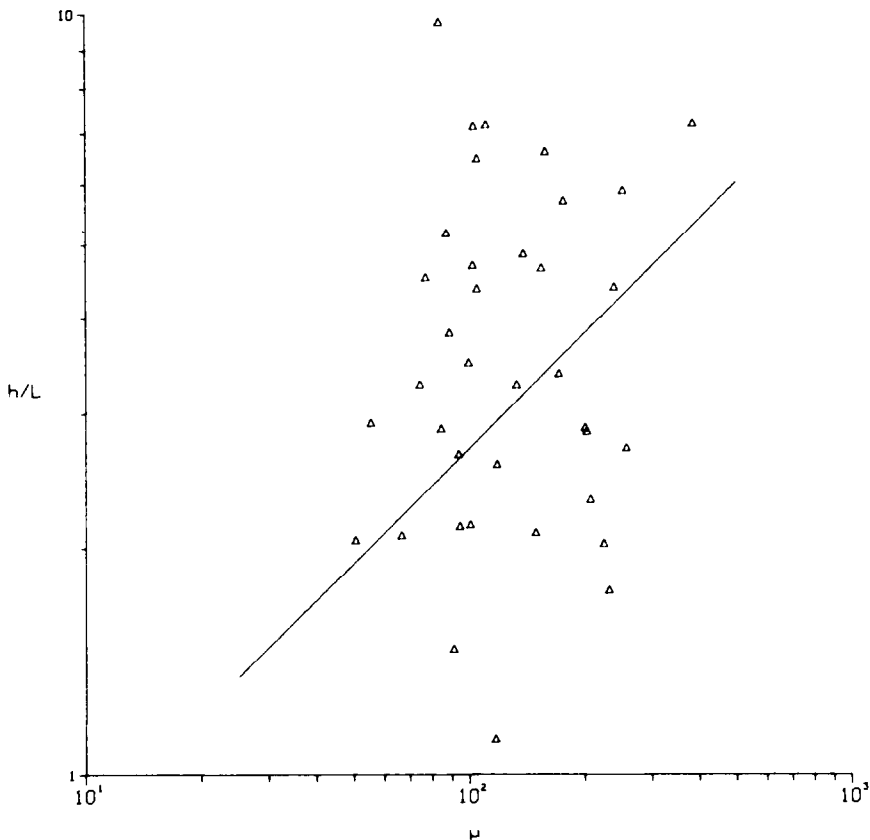


Fig. 4(c). Same as Figure 4(b), but with the Wangara data.

case study of the nocturnal boundary layer, Nieuwstadt and Driedonks (1979) conclude that advection effects are important, especially in the upper part of the boundary layer, and explain the differences between their observed and calculated results in terms of temperature advection.

A more recent analysis of the Minnesota stable data (Caughey *et al.*, 1978) and the acoustic sounder data at the 200 m high meteorological tower at Cabauw in the Netherlands (Nieuwstadt and Driedonks, 1979) tend to support Equation (9), though the value of the constant  $a$  still remains unsettled.

Another parameterization for  $h$  can be obtained by integrating the equations of motion (1) over the mixing-layer depth in the steady-state limit. This yields the constraints,

$$\int_{z_0}^h (V - V_g) dz = \frac{1}{f} \int_{z_0}^h \frac{\partial \overline{uw}}{\partial z} dz = u_*^2/f, \quad (10)$$

$$\int_{z_0}^h (U_g - U) dz = \frac{1}{f} \int_{z_0}^h \frac{\partial \overline{vw}}{\partial z} dz = 0. \quad (11)$$

The latter indicates that  $U$  must overshoot  $U_g$  within the mixing layer. We can write the first constraint, to a good approximation, as

$$u_*^2/f \propto - \int_{z_0}^h V_g dz = hG \sin \alpha, \quad (12)$$

or

$$h = a_1 u_*^2 / (fG \sin \alpha).$$

This can also be expressed as

$$u_* / G = a_2 (fh \sin \alpha / G)^{1/2} \quad (13)$$

where  $a_2 = a_1^{-1/2}$ . The last relation, shown as the dashed line in Figure 5, fits the model predictions well with the constants  $a_2 = 0.80$  and  $a_1 = 1.56$ ; these values agree with  $a_2 = 0.79$  and  $a_1 = 1.6$  obtained by Brost and Wyngaard (1978) from a different model.

### 3.3. GEOSTROPHIC DRAG AND HEAT TRANSFER RELATIONS

Asymptotic matching of the similarity profiles of mean velocity and temperature in the inner and outer layers of the stable PBL leads to the well-known geostrophic drag

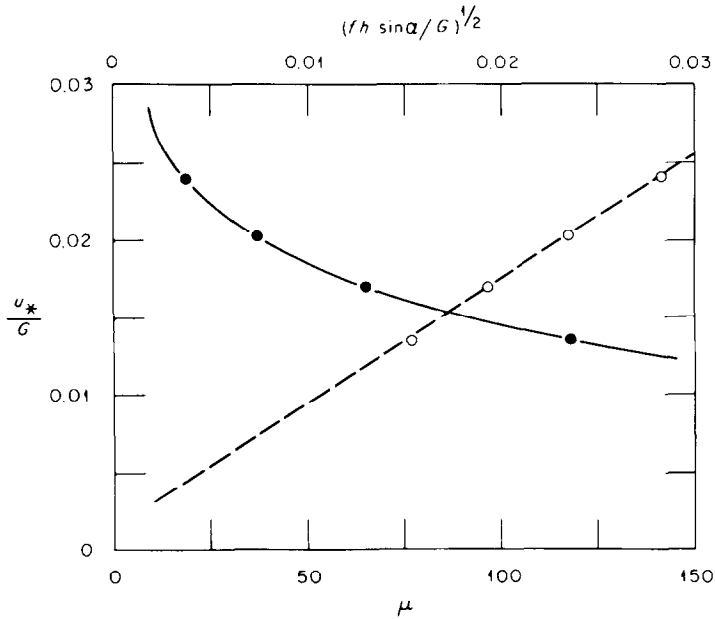


Fig. 5. Calculated variation of the geostrophic drag coefficient in the nocturnal PBL as a function of  $(fh \sin \alpha / G)^{1/2}$ , indicated by dashed line, and the stability parameter  $\mu$ , indicated by solid line, for  $Ro \approx 10^7$ .

and heat transfer relations:

$$G \cos \alpha / u_* = \frac{1}{k} \{ \ln |u_* / fz_0| - A(\mu) \}$$

$$G \sin \alpha / u_* = \frac{B(\mu)}{k} \text{sign}(f) \quad (14)$$

$$(\Theta_h - \Theta_0) / \theta_* = \frac{0.74}{k} \{ \ln |u_* / fz_0| - C(\mu) \}$$

where  $\Theta_h$  is the potential temperature at the top of the boundary layer, and  $A$ ,  $B$ , and  $C$  are universal functions of  $\mu$  to be determined from theory and observations. The first two equations may be combined to give an implicit relation between the geostrophic drag coefficient,  $C_g = u_* / G$ , and the surface Rossby number,  $Ro = |G / fz_0|$ , as follows:

$$\ln Ro = A(\mu) - \ln C_g + \left[ \frac{k^2}{C_g^2} - B^2(\mu) \right]^{1/2} \quad (15)$$

which implies that  $u_* / G = C_g(Ro, \mu)$ ; for a given Rossby number,  $C_g$  should only depend on  $\mu$ . Figure 5 (solid line) shows the variation of the geostrophic drag coefficient with  $\mu$  in the present model ( $Ro \approx 10^7$ ).

The functions  $A(\mu)$ ,  $B(\mu)$  and  $C(\mu)$ , calculated from Equation (14) in the model, are shown in Figure 6 where they are compared with the best-fit polynomial

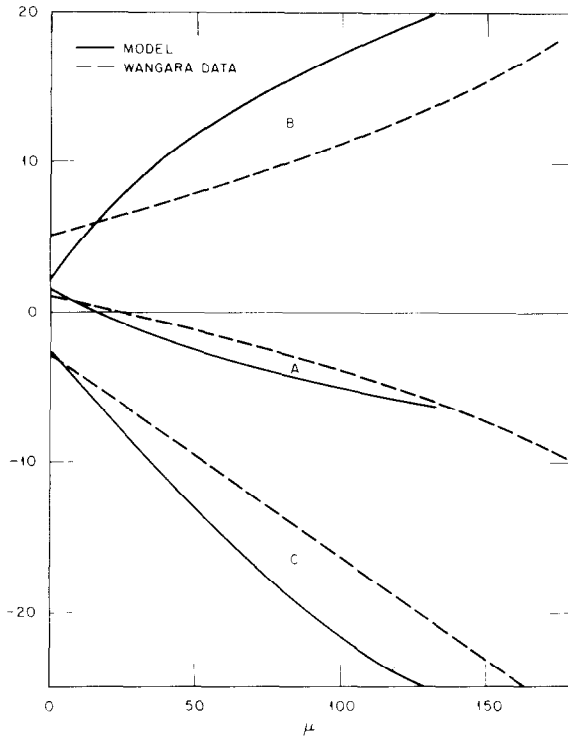


Fig. 6. Comparison of calculated similarity functions  $A$ ,  $B$ , and  $C$  in the geostrophic drag and heat transfer relations with the best-fits to the Wangara stable PBL data.

expressions to the Wangara data (Clarke *et al.*, 1971) given by Arya (1975). There is fair agreement between model predictions and observations. From Equations (9), (12), and (14), we can write  $B(\mu) = b_1\mu^{1/2}$  where the constant  $b_1 = 1.71$ . For  $\mu > 10$ , the present model results can be represented by the best-fit expressions shown in Table I, where they are compared with the functions given by Arya (1977), Briggs (1977), and Brost and Wyngaard (1978), all obtained from different models of the stable barotropic PBL. Except for  $B(\mu)$ , the agreement between various models is good.

TABLE I  
Comparison of PBL similarity functions  $A$ ,  $B$ , and  $C$  from different models

	$A(\mu)$	$B(\mu)$	$C(\mu)$
Present model	$\ln \mu^{1/2} - 0.98\mu^{1/2} + 2.5$	$1.79\mu^{1/2} - 0.6$ or $1.71\mu^{1/2}$	$\ln \mu^{1/2} - 3\mu^{1/2} + 6.5$
Arya (1977)	$\ln \mu^{1/2} - 0.96\mu^{1/2} + 2.5$	$1.15\mu^{1/2} + 1.1$	$\ln \mu^{1/2} - 3\mu^{1/2} + 7.0$
Briggs (1977)	$\ln \mu^{1/2} - 1.0\mu^{1/2} + 2.5$	$1.86\mu^{1/2}$	—
Brost & Wyngaard (1978)	$\ln \mu^{1/2} - 0.9\mu^{1/2} + 2.0$	$1.40\mu^{1/2}$	—

## Acknowledgments

This work was performed under an agreement between the National Oceanic and Atmospheric Administration and the Department of Energy. We gratefully acknowledge several helpful discussions with G. A. Briggs of ATDL.

## References

- Arya, S. P. S.: 1975, 'Geostrophic Drag and Heat Transfer Relations for the Atmospheric Boundary Layer', *Quart. J. Roy. Meteorol. Soc.* **101**, 147–161.
- Arya, S. P. S.: 1977, 'Suggested Revisions to Certain Boundary Layer Parameterization Schemes used in Atmospheric Circulation Models', *Mon. Wea. Rev.* **105**, 215–227.
- Blackadar, A. K.: 1957, 'Boundary Layer Wind Maxima and their Significance for the Growth of Nocturnal Inversions', *Bull. Amer. Meteorol. Soc.* **38**, 283–290.
- Blackadar, A. K.: 1976, 'Modeling the Nocturnal Boundary Layer', *Third Symposium on Atmospheric Diffusion and Air Quality*, Raleigh (Oct. 1976), pp. 46–49, Preprints, Amer. Meteorol. Soc., Boston.
- Briggs, G. A.: 1977, 'Predictions of Nocturnal Mixing Layer Parameters', *Manuscript*, 40pp., ATDL, Oak Ridge, Tenn.
- Brost, R. A. and Wyngaard, J. C.: 1978, 'A Model Study of the Stably Stratified Planetary Boundary Layer', *J. Atmos. Sci.* **35**, 1427–1440.
- Businger, J. A., Wyngaard, J. C., Izumi, Y., and Bradley, E. F.: 1971, 'Flux-Profile Relations in the Atmospheric Surface Layer', *J. Atmos. Sci.* **28**, 181–189.
- Businger, J. A.: 1973, 'Turbulent Transfer in the Atmospheric Surface Layer', in D. A. Haugen (ed.), *Workshop on Micrometeorology*, Amer. Meteorol. Soc., Boston, pp. 101–149.
- Businger, J. A. and Arya, S. P. S.: 1974, 'The Height of the Mixed Layer in the Stably Stratified Planetary Boundary Layer', *Adv. in Geophys.* **18A**, Academic Press, New York, 73–92.
- Caughey, S. J., Wyngaard, J. C., and Kaimal, J. C.: 1978, 'Turbulence in the Evolving Stable Boundary Layer', *Manuscript*, 46 pp., CIRES, Univ. of Colorado / NOAA, Boulder.
- Clarke, R. H., Dyer, A. J., Brook, R. R., Reid, D. G., and Troup, A. J.: 1971, 'The Wangara Experiment: Boundary Layer Data', Tech. Pap. No. 19, CSIRO, Div. Meteor. Phys., Melbourne, Australia, 362 pp.
- Deardorff, J. W.: 1972, 'Rate of Growth of the Nocturnal Boundary Layer', in H. W. Church and R. E. Luna (eds.) *Proc. of the Symposium on Air Pollution, Turbulence and Diffusion*, New Mexico (Dec. 1971), pp. 183–190.
- Delage, Y.: 1974, 'A Numerical Study of the Nocturnal Atmospheric Boundary Layer', *Quart. J. Roy. Meteorol. Soc.* **100**, 351–364.
- Izumi, Y.: 1971, 'Kansas 1968 Field Program Data Report', *AFCRL-72-0041*, 79 pp., AFGL, Hanscom Field, Bedford, Mass.
- Izumi, Y. and Barad, M.: 1963, 'Wind and Temperature Variations during Development of a Low-Level Jet', *J. Appl. Meteorol.* **2**, 668–673.
- Melgarejo, J. W. and Deardorff, J. W.: 1975, 'Revision to "Stability Functions for the Boundary-Layer Resistance Laws Based upon Observed Boundary-Layer Heights"', *J. Atmos. Sci.* **32**, 837–839.
- Nieuwstadt, F. T. M. and Driedonks, A. G. M.: 1979, 'The Nocturnal Boundary Layer: a case study compared with model calculations', *Manuscript*, Royal Netherlands Meteorological Institute, De Bilt, 35pp.
- Rao, K. S. and Snodgrass, H. F.: 1978, 'The Structure of the Nocturnal Planetary Boundary Layer', *ATDL Contribution File No. 78/9*, NOAA, Oak Ridge, Tenn., 44pp.
- Wyngaard, J. C.: 1975, 'Modeling the Planetary Boundary Layer - Extension to the Stable Case', *Boundary-Layer Meteorol.* **9**, 441–460.
- Yamada, Y.: 1976, 'On the Similarity Functions A, B, and C of the Planetary Boundary Layer', *J. Atmos. Sci.* **33**, 781–793.
- Yu, T. W.: 1978, 'Determining the Height of the Nocturnal Boundary Layer', *J. Appl. Meteorol.* **17**, 28–33.

- Zeman, O. and Lumley, J. L.: 1978, 'Buoyancy Effects in Entraining Turbulent Boundary Layers: A Second-order Closure Study', *Proceedings of Symposium on Turbulent Shear Flows*, Springer-Verlag (to appear).
- Zilitinkevich, S. S.: 1972, 'On the Determination of the Height of the Ekman Boundary Layer', *Boundary-Layer Meteorol.* **3**, 141-145.
- Zilitinkevich, S. S.: 1975, 'Resistance Laws and Prediction Equations for the Depth of the Planetary Boundary Layer,' *J. Atmos. Sci.* **32**, 741-752.